ELSEVIER

International Journal of Heat and Fluid Flow 20 (1999) 614–623

International Journal of HEAT AND FLUID FLOW

www.elsevier.com/locate/ijhff

Laminar natural convection in a fully partitioned enclosure containing fluid with nonlinear thermophysical properties

D.M. Cuckovic-Dzodzo [a], M.B. Dzodzo [b,*], M.D. Pavlovic [c]

[a] *Computer Learning Center, Monroeville Branch, Pittsburgh, PA, USA*

[b] *Westinghouse Electric Company, Science and Technology Department, M/S 401-2A6, 1344 Beulah Road, Pittsburgh, PA 15235-5083, USA*

[c] *Mechanical Engineering Department, University of Belgrade, Belgrade, Yugoslavia*

Received 8 May 1998; accepted 20 June 1999

Abstract

The effects of a heat conducting partition on the laminar natural convection heat transfer and fluid flow were obtained by comparing the numerical and experimental results for a cubic enclosure without and with a partition. The two opposite vertical walls of the enclosure were isothermal at different temperatures. The working fluid was glycerol. The complete vertical partition, made of Plexiglass, was positioned in the middle of the enclosure. The visualizations of the velocity and temperature fields were obtained by using respectively, Plexiglass and liquid crystal particles as tracers. A middle plane perpendicular to the partition was numerically modeled. The steady two-dimensional model accounted for the variable thermophysical properties of the fluid. The finite volume method based on the finite difference approach was applied. The convective terms were approximated using a deferred correction central difference scheme. The velocity and temperature fields and the distribution of the local and average Nusselt numbers were found as a function of the Rayleigh ($38\,000 < Ra < 369\,000$) and Prandtl ($2700 < Pr < 7000$) numbers.

Keywords: Laminar natural convection; Cubic enclosure; Conductive partition; Thermophysical properties

Notation

b	width of the partition, $b = 0.002$ (m)
c_p	specific heat of the fluid (J/kg K)
D	depth of the enclosure, $D = 0.038$ (m)
g	acceleration due to gravity (m/s^2)
H	height of the enclosure, $H = 0.038$ (m)
k_f	thermal conductivity of the fluid (W/mK)
k_p	thermal conductivity of the partition (W/mK)
N	number of partitions
Nu	local Nusselt number
$\overline{Nu}$	average Nusselt number
p	pressure (N/m^2)
Pr	Prandtl number based on T_0, $Pr = \nu/\alpha$
Pr_h	Prandtl number based on T_h
Pr_c	Prandtl number based on T_c
Ra	Rayleigh number, $Ra = g\beta(T_h - T_c)W^3/\nu\alpha$, properties are based on T_0
Ra_H	Rayleigh number based on H, $Ra_H = g\beta(T_h - T_c)H^3/\nu\alpha$
T	temperature (°C)
T_C	temperature (°C)
T_c	temperature of the cold vertical wall (°C)
T_h	temperature of the hot vertical wall (°C)
T_K	temperature (K)
T_0	average temperature $T_0 = (T_h + T_c)/2$ (°C)
V	velocity vector (m/s)
u	velocity along x (m/s)
v	velocity along y (m/s)
W	width of the enclosure, $W = 0.038$ (m)
Greek	
α	thermal diffusivity $\alpha = k_f/\rho c_p$ (m^2/s)
β	thermal expansion coefficient of the fluid (1/K)
ρ	density of the fluid (kg/m^3)
λ	conductive resistance ratio, $\lambda = (W/k_f)/(b/k_p)$
ν	kinematic viscosity of the fluid (m^2/s)
μ	dynamic viscosity of the fluid (kg/m s)

1. Introduction

Natural convection in enclosures has been receiving considerable attention due to its numerous applications such as in solar collectors, thermal design of buildings, nuclear reactor design and cooling of electronic equipment.

Convective flow in enclosures without a partition is very well studied. One of the first experimental and numerical studies was presented by Elder (1965a,b, 1966). An overview of later results was presented by Ostrach (1972, 1982), Catton (1978) and Yang (1987).

* Corresponding author. Tel.: +1-412-256-1655; fax: +1-412-256-1190.

E-mail address: dzodzomb@westinghouse.com (M.B. Dzodzo)

0142-727X/99/$ - see front matter
PII: S0142-727X(99)00053-3

Results of natural convection in enclosures are also used as bench mark data for validation of various numerical methods for solving Navier–Stokes equations. A comparison of 37 numerical results (from various authors) for two-dimensional air-filled ($Pr = 0.71$) square cavities and opposite vertical walls at different temperatures was presented by de Vahl Davis and Jones (1983) and de Vahl Davis (1983). The bench mark numerical results were obtained with grids up to 81×81 points at Rayleigh numbers of 10^3, 10^4 , 10^5 and 10^6. Hortmann et al. (1990) presented numerical results of the same problem for $Ra = 10^4$, 10^5 and 10^6, using 640×640 control volume cells. At $Ra = 10^3$ isotherms are parallel to the vertical walls and conductive heat transfer dominates. The horizontal temperature gradient generates a single vortex in the center of the enclosure. The effects of convection at $Ra = 10^4$ create stronger temperatu\re gradients near the vertical walls, a stratified core in the cavity and an elliptical vortex shape. Convective heat transfer in the boundary layers near the vertical walls dominates at $Ra = 10^5$. Horizontal temperature gradients in the center of the cavity are close to zero and in different directions. As a consequence, two vortices are present in the core. Further increase of the Rayleigh number decreases the thickness of the boundary layers and moves the two vortices closer to the vertical walls. A third vortex appears in the center of the cavity at $Ra = 10^6$. As convection becomes dominant the average Nusselt number increases from 1.116 to 2.245 to 4.522 to 8.825, passing through $Ra = 10^3$, 10^4, 10^5 and 10^6, respectively.

Laminar natural convection in enclosures with partitions attracts attention because including partitions is one way to decrease heat transfer in various engineering applications. The problem was treated experimentally by Duxbury (1979), and Nakamura et al. (1984), where the working fluid was air. Anderson and Bejan (1981), and Nishimura et al. (1987, 1988), used water as working fluid. Nakamura et al. (1984), also included radiation effects.

The same problem was investigated analytically by Anderson and Bejan (1981), Nakamura et al. (1984), Acharya and Tsang (1985), Tong and Gerner (1986), Ho and Yih (1987), Nishimura et al. (1987, 1988), Kangni et al. (1991), Ciofalo and Karayiannis (1991), Karayiannis et al. (1992) and Mamou et al. (1994).

According to Nakamura et al. (1984), results obtained by Duxbury (1979) and Nakamura et al. (1984) based on the assumption of isothermal partition indicated that the average Nusselt number for the enclosure with partitions is proportional to $(N+1)^{-5/4}$.

An enclosure with a thin ($b = 0$) partition was studied numerically by Acharya and Tsang (1985) for Rayleigh numbers up to 10^7, enclosure inclination angles of 30°, 45°, 60° and 90°, aspect ratios H/W of 0.5 and 1 and air as the working fluid ($Pr = 0.7$). The average Nusselt number is reduced 45–50% by partitioning the enclosure. The partition temperature nonuniformity increases with Rayleigh number. For a vertical enclosure, the partition temperature increases almost linearly along its length. The effects of the position of one thin vertical partition on the convective heat transfer were studied by Tong and Gerner (1986) by using finite difference methods. Air-filled ($Pr = 0.71$) rectangular enclosures with aspect ratios H/W of 5, 10 and 15 and Rayleigh numbers 10^4 and 10^5 were studied. It was concluded that the greatest reduction in heat transfer occurs by positioning the partition in the center of an enclosure. In some cases a partition reduces heat transfer more than 50%.

Anderson and Bejan (1981) reported analytical and experimental results for heat transfer in a rectangular enclosure with aspect ratio $H/W = 0.3$ and a thin single or double vertical partitions. Experiments were performed with water, in the range of Rayleigh numbers $10^9 < Ra_H < 10^{10}$. The average Nusselt number is proportional to $(1 + N)^{-0.61}$.

Nishimura et al. (1988) studied, both experimentally and numerically, the effect of multiple thin partitions. The working fluid was water ($Pr = 6$). The experiments were performed in enclosures with $H/W = 4$ and 10, for the range $10^6 < Ra < 10^8$ and the number of partitions was from $N = 1$ to 4. Numerical results were obtained for $H/W = 4$, $N = 2$ and 3, and the range of Rayleigh numbers $10^4 < Ra < 10^7$. It was concluded that the average Nusselt number is inversely proportional to $(1 + N)$.

The conjugated heat transfer in an air-filled ($Pr = 0.7$) rectangular enclosure with a thick ($b > 0$) conductive vertical partition positioned in the middle was analyzed numerically by Ho and Yih (1987). The results were obtained for four different aspect ratios $H/W = 1$, 2, 5 and 10, range of Rayleigh numbers $10^3 < Ra < 10^6$ and the conductive resistance ratio up to $\lambda = 50\,000$. It was found that for $\lambda > 200$ the horizontal temperature gradient across the partition wall is negligible. A peak value of the average Nusselt number is detected for $100 < \lambda < 300$, Rayleigh numbers $Ra \geqslant 10^5$ and aspect ratio $H/W \geqslant 2$. After reaching a maximum, the average Nusselt numbers decrease and become constant for $\lambda > 10^4$, for all Rayleigh numbers and aspect ratios. It was found that in some cases the partition reduced the average Nusselt number up to 60%. With an increased enclosure aspect ratio the centers of the vortices in the separate halves tend to be closer to the enclosure diagonal.

Kangni et al. (1991) studied conjugated heat transfer in enclosures with multiple partitions (N varied from 1 to 5), aspect ratio H/W from 5 to 20, partition thickness b/W from 0.01 to 0.1, various partition positions, thermal conductivity ratio of partition to fluid k_p/k_f from 1 to 10^4, range of Rayleigh numbers $10^3 < Ra < 10^7$, and $Pr = 0.72$. It was found that the maximum of the average Nusselt number exists for a given conductivity ratio k_p/k_f. Increasing the aspect ratio and positioning the partition in the center is the most effective method of reducing the heat transfer.

Effects of partial and complete vertical partitions positioned in the middle of rectangular enclosures were studied numerically by Ciofalo and Karayiannis (1991), while a detailed analysis of the case with a complete vertical partition was presented by Karayiannis et al. (1992). The thickness and conductivity of the enclosure were varied, as well as, the aspect ratio of the enclosure (H/W from 0.1 to 16). Rayleigh numbers were from 3.5×10^3 to 3.5×10^7 for a nonpartitioned enclosure and from 10^5 to 1.6×10^8 for a partitioned enclosure filled with air ($Pr = 0.72$). The results were obtained with adiabatic or linear temperature profile boundary conditions for the horizontal end walls. The average Nusselt numbers for various cases were presented in graphic form. It was found that the difference between average Nusselt numbers calculated for a real partition (with thickness $b > 0$ and conductivity k_p) and an ideal partition ($b = 0$ and isothermal) is not greater than 12% for the case of adiabatic horizontal end walls.

Mamou et al. (1994) studied analytically and numerically the influence of multiple, thick and conductive partitions inside inclined rectangular enclosures filled with air ($Pr = 0.71$), with a uniform heat flux at the side walls and two other walls adiabatic. In the case of a vertical enclosure the average Nusselt numbers are proportional to $(1 + N)^{-8/9}$. With increasing conductivity ratio k_p/k_f the heat transfer first increases, then reaches a maximum and then decreases. The maximum average Nusselt number occurs at a lower conductivity ratio as the number of partitions increases.

In most of the presented papers the working fluid used was air ($Pr = 0.71$), but in some cases water was used as well. The Boussinesq approximation was used for all numerical models. The density was linearly dependent on the temperature only in the buoyancy force term while the thermophysical properties were considered to be constant (taken for an average fluid temperature). The Boussinesq approximation, with air or water as the working fluid, produces a small discrepancy with the experimental results if the temperature difference between the opposite vertical walls is not great (see Gray and Giogini (1976)). In order to avoid this limitation the Boussinesq approximation was not applied to the present numerical model. Instead, the fluid properties were dependent on temperature.

In the present paper glycerol has been used as a working fluid. The coefficient of the dynamic viscosity of glycerol is nonlinearly dependent on temperature. It can decrease by an order of magnitude between the temperatures of the opposite walls. Laminar natural convection in cubic enclosures without and with partitions was studied experimentally and numerically. The temperature and velocity fields were visualized experimentally by using thermochromic liquid crystals and white colored Plexiglass particles, respectively, as tracers. Equations with variable glycerol properties were used instead of the Boussinesq approximation.

Application of the particular fluid and enclosure properties used in the experiment for a mathematical model caused the loss of generality, but made it possible to capture effects of the nonlinear property variations and offered better agreement between the experimental and numerical results. Once developed, the numerical model (which takes into account nonlinear variations of the fluid properties) could be applied to other fluids and enclosure configurations.

The velocity and temperature fields are presented for a range of Rayleigh and Prandtl numbers. The effects of partition on the decrease of heat transfer were obtained by comparing the local and average Nusselt numbers for the enclosures without and with partition.

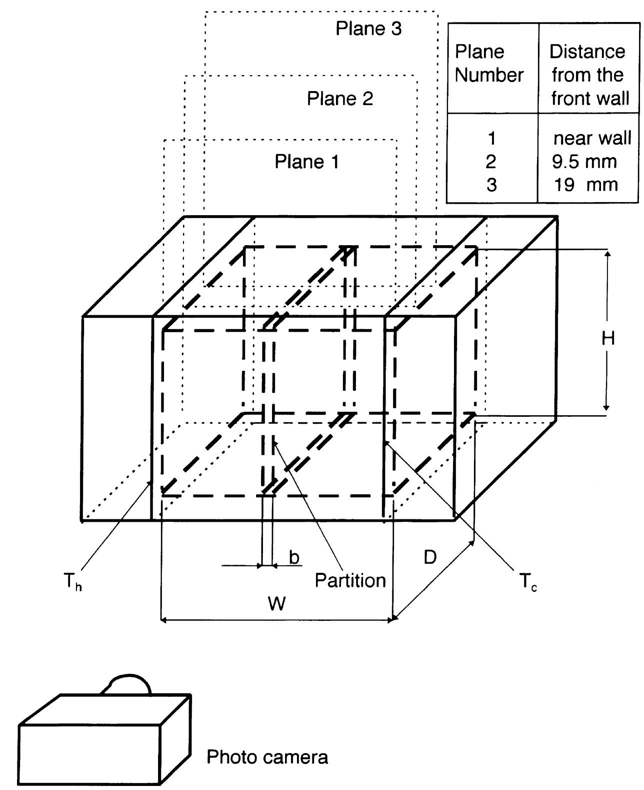

Fig. 1. Schematic of the enclosure with partition and illuminated vertical cross-sections.

2. Experimental methods

Two experimental installations were used to perform the experimental work, the first at the University of Belgrade and the second at the University of Akron. In both cases planes of light were used to illuminate various cross-sections of the enclosure (see Fig. 1). The photographic records were taken for each cross-section.

The dimension of the enclosure was 38 × 38 × 38 mm. The walls and partition were made of transparent Plexiglass 8 mm and 2 mm thick, respectively. Two opposite vertical walls were made of thick aluminum plates (anodized in black). Water from thermal baths at different temperatures circulated through channels (drilled inside the walls) and maintained the aluminum vertical walls isothermal at different temperatures.

The first experimental installation was similar to the one described by Hiller et al. (1989). The details of the installation were presented in Dzodzo, (1993). This installation was used to map velocity fields by using white colored Plexiglass particles and to perform a preliminary visualization of temperature fields using a volumetric concentration of 0.08% of unencapsulated liquid crystals (type TM216 by BDH Chemicals, 1989). Despite the density of the liquid crystals being smaller than that of glycerol (whose density ranged from 1263 to 1241 kg/m^3 for temperatures of 20°C to 58°C, respectively) it was noticed by Dzodzo (1993) that entrained liquid crystal particles have the same velocity as the buoyancy neutral particles of Plexiglas (density 1190 kg/m^3). The frequency of the flashing light was controlled by a computer, so that the velocities of the tracer particles could be obtained from their consecutive positions. The main sources of velocity uncertainty were in establishing the positions of the centers of the tracer particles and their distance from the vertical walls, due to light reflection from the tracer particles and enclosure internal walls, respectively. Time intervals between lamp flashes and the camera aperture were adjusted so that the velocity uncertainty is less than ±0.00001 m/s. The particle position uncertainty relative to the internal walls was ±0.15 mm.

The second installation was used to map temperature fields by using a higher concentration (approximately 0.25%) of encapsulated liquid crystals. The details of the installation were presented in Dzodzo et al., (1994). A Xenon lamp provided a continuous plane of light. The tracers of the liquid crystals and images for the temperature fields were obtained by using a longer exposure time of the photo camera. In the portions of the partitioned enclosure near the hot (left) and cold (right) aluminum walls the encapsulated liquid crystals BM100/R40C20W/S33 and BM100/R22C20W/S33 (see Hallcrest, 1991 and Parsley, 1991) were used, respectively. According to the producer's specification these crystals have sizes in the range of 100 μm in diameter. They start reflecting the color red around 40°C and 22°C, respectively and pass through the color spectrum over a 20°C span. The calibration results of the temperatures versus colors of the liquid crystals were obtained by Lattime (1995) and presented in (Lattime et al., 1995). These results showed that the uncertainty of the temperature measurement could be ±0.15°C in the range of red to light blue reflected colors and ±0.46°C beyond the light blue color. According to the calibration results the first and second type of crystals reflect red, yellow and green colors at 38.4°C, 38.6°C, 39.2°C and 20.9°C, 21.2°C, 21.6°C, respectively. To reduce the experimental uncertainty, the experiment was performed using the same calibrated thermocouples and mercury thermometers (with 0.1°C resolution), thermal baths and aluminum plates, as employed in the color–temperature calibration. The nonuniformity of the aluminum plates' surface temperatures was checked with a contact thermometer. There was less than 0.1°C difference between the surface temperature and water in the aluminum plate channels and thermal baths.

This is due to the high flow rates of water through the channels inside the aluminum plates and high heat conductivity of aluminum.

The comparison of the temperature and velocity fields in three planes (for the same partitioned enclosure as in Fig. 1) presented by Cuckovic-Dzodzo (1996) and Cuckovic-Dzodzo et al. (1996b) showed good agreement of the temperature and velocity fields in the planes 2 and 3 (9.5 and 19 mm distant from the front wall, respectively). This provided an opportunity to model only the middle vertical plane numerically, as a two-dimensional case. This is in agreement with Penot and N'Dame (1992) conclusion that the aspect ratio in the cavity depth direction needs to be greater than 1.8 for the two-dimensional assumption to be valid. However, in the case of an enclosure without partition the aspect ratio is equal to one, and a discrepancy between numerical and experimental results due to three dimensional effects could be present, especially in the range of Rayleigh numbers $10^4 < Ra < 10^5$, due to the transition from a one vortex to a two vortex flow pattern.

3. Numerical method

A two-dimensional numerical simulation of natural convection in the middle vertical plane 3 was performed by assuming that the influences of the front and back walls were negligible on the flow in the middle cross-section. The equations for *a* fluid with variable properties were used. The continuity and momentum equations are

$$\frac{\partial}{\partial x}\rho u + \frac{\partial}{\partial y}\rho v = 0, \tag{1}$$

$$\frac{\partial}{\partial x}\rho uu + \frac{\partial}{\partial y}\rho vu = \frac{\partial}{\partial x}\left[2\mu\frac{\partial u}{\partial x} - \frac{2}{3}\mu(\nabla V)\right] + \frac{\partial}{\partial y}\left[\mu\left(\frac{\partial u}{\partial y} + \frac{\partial v}{\partial x}\right)\right] - \frac{\partial p}{\partial x}, \tag{2}$$

$$\frac{\partial}{\partial x}\rho uv + \frac{\partial}{\partial y}\rho vv = \frac{\partial}{\partial x}\left[\mu\left(\frac{\partial v}{\partial x} + \frac{\partial u}{\partial y}\right)\right] + \frac{\partial}{\partial y}\left[2\mu\frac{\partial v}{\partial y} - \frac{2}{3}\mu(\nabla V)\right] - \frac{\partial p}{\partial y} + \rho g. \tag{3}$$

The energy equation for the fluid is

$$\frac{\partial}{\partial x}\rho u c_p T + \frac{\partial}{\partial y}\rho v c_p T = \frac{\partial}{\partial x}\left(k_{\mathrm{f}}\frac{\partial T}{\partial x}\right) + \frac{\partial}{\partial y}\left(k_{\mathrm{f}}\frac{\partial T}{\partial y}\right), \tag{4}$$

while the energy (conduction) equation for the partition wall reads

$$\frac{\partial}{\partial x}\left(k_{\mathrm{p}}\frac{\partial T}{\partial x}\right) + \frac{\partial}{\partial y}\left(k_{\mathrm{p}}\frac{\partial T}{\partial y}\right) = 0. \tag{5}$$

The boundary conditions are presented in Fig. 2. The horizontal walls were assumed to be adiabatic with the vertical walls being at different isothermal temperatures. The conjugate heat transfer boundary conditions were applied at both sides of the vertical partition.

The properties of the glycerol were specified as functions of temperature as follows:

$$\rho = 9.597 \times 10^{-4} T_{\mathrm{C}}^2 - 0.6542 T_{\mathrm{C}} + 1276.0, \tag{6}$$

$$\beta = 0.002266667 \times 10^{-4} T_{\mathrm{C}} + 4.53133 \times 10^{-4}, \tag{7}$$

$$\mu = -1.63289 \times 10^{-8} T_{\mathrm{C}}^5 + 4.129 \times 10^{-6} T_{\mathrm{C}}^4 - 4.238 \times 10^{-4} T_{\mathrm{C}}^3 + 0.02241 T_{\mathrm{C}}^2 - 0.62486 T_{\mathrm{C}} + 7.6358, \tag{8}$$

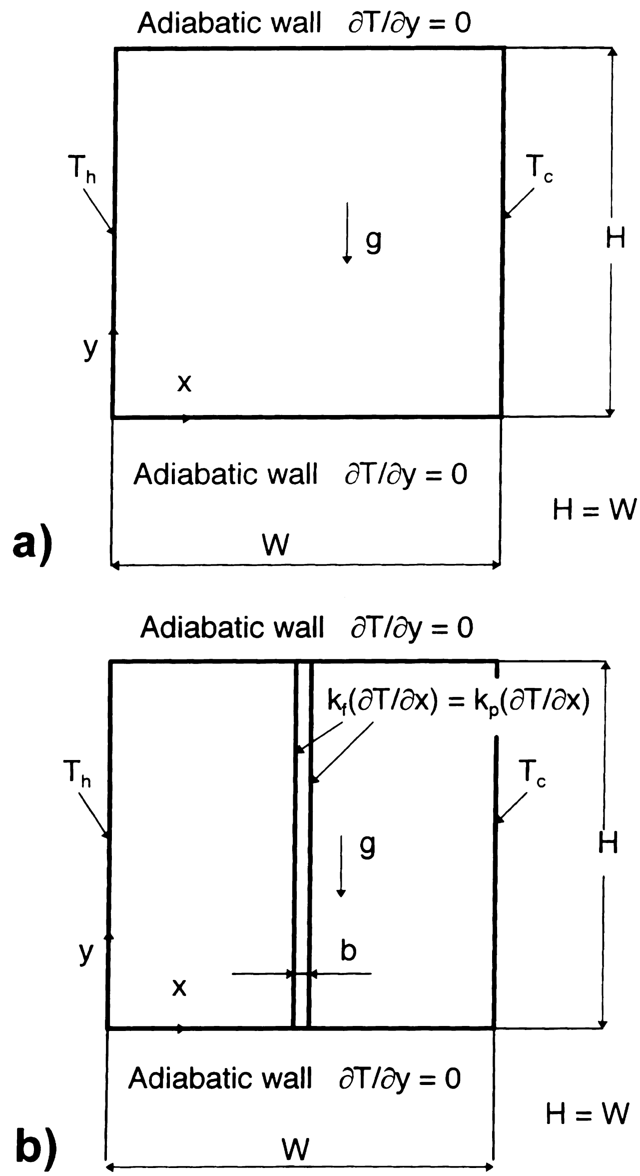

Fig. 2. Numerical models of the middle plane of the enclosures: (a) wihout partition and (b) with conducting partition.

$$k_{\mathrm{f}} = 0.2484397 + 1.318422 \times 10^{-4} T_{\mathrm{K}}, \tag{9}$$

$$c_p = 0.412731 \times 10^3 + 7.89332 T_{\mathrm{K}} - 5.71088 \times 10^{-3} T_{\mathrm{K}}^2 + 4.31645 \cdot 10^{-6} \times T_{\mathrm{K}}^3, \tag{10}$$

where T_{C} and T_{K} are temperatures in Celsius and Kelvin degrees, respectively. Eqs. (6)–(8) for density, coefficient of volumetric expansion and dynamic viscosity were obtained experimentally (Dzodzo 1991), while Eqs. (9) and (10) for the coefficient of conductivity and the specific heat of glycerol were taken from (Toulokian et al., 1970a) and (Toulokian and Makita, 1970), respectively. The thermal conductivity of the Plexiglass partition was 0.195 W/mK (Toulokian et al., 1970b). Eqs. (6)–(8) can be applied for temperatures between 20° and 60°C. It should be noted that the dynamic viscosity of glycerol with a small content of water (introduced together with the liquid crystals) is lower than for pure glycerol. Eq. (8) is for the dynamic viscosity of applied glycerol mixed with liquid crystals. However, due to the different contents of water intro-

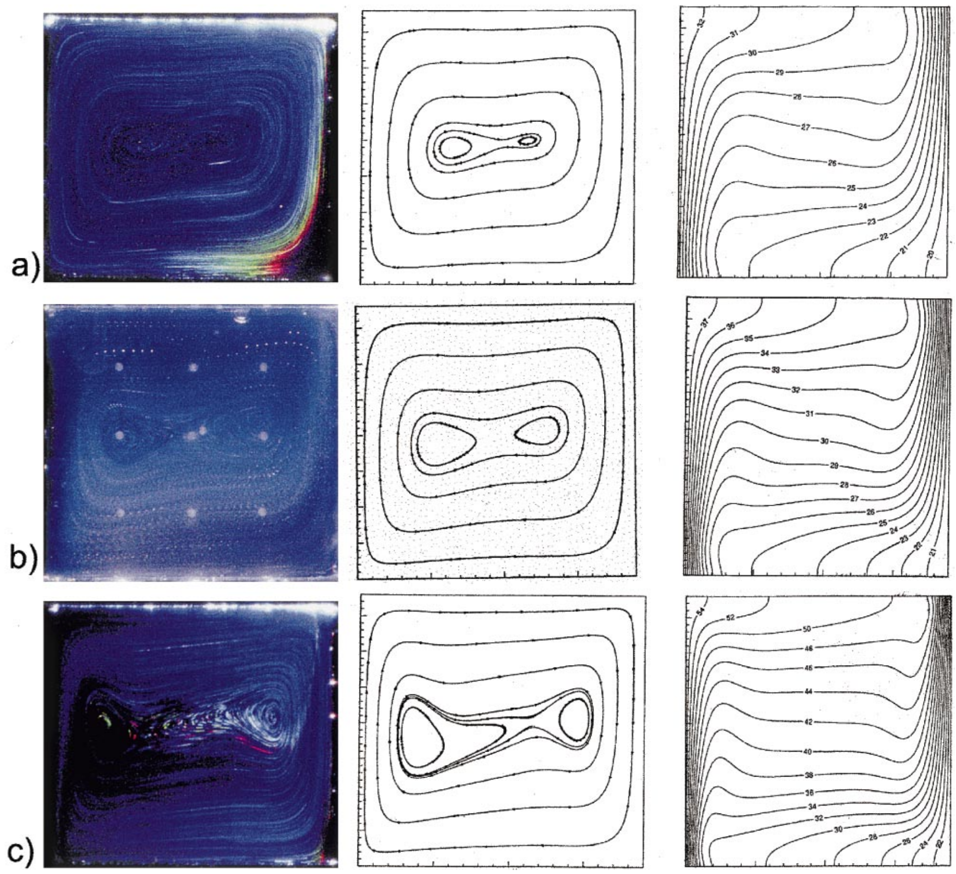

Fig. 3.

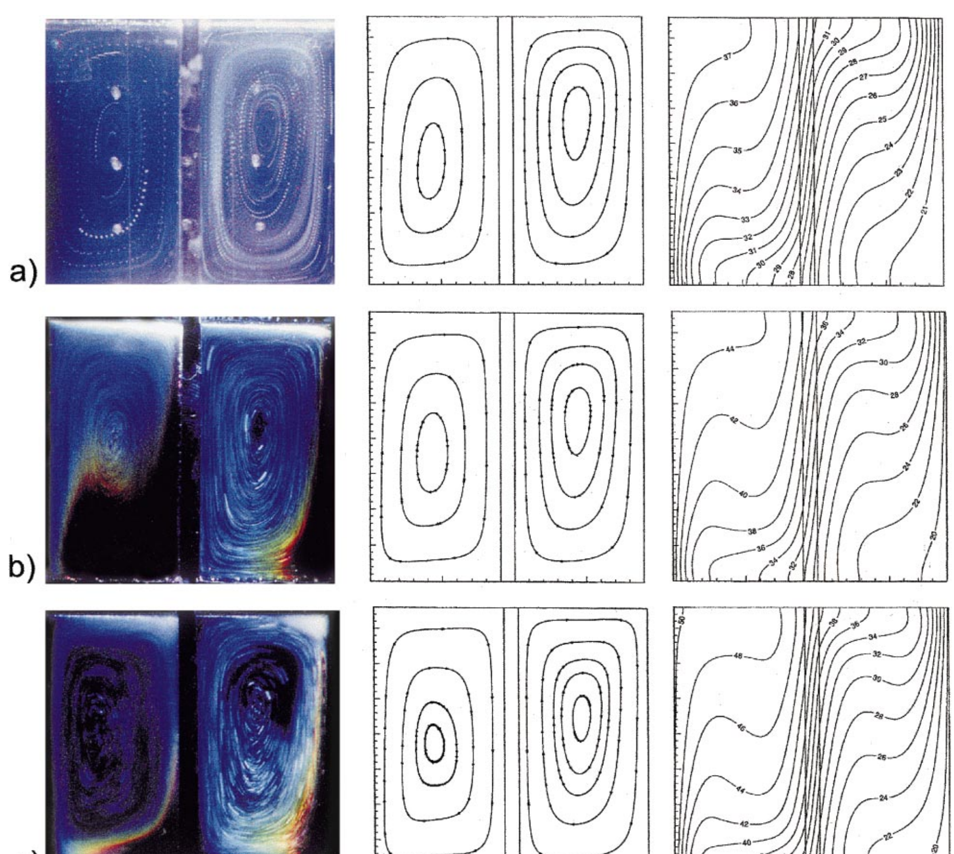

Fig. 4.

Fig. 3. Experimental and numerical results for the enclosure without partiition: (a) $Ra = 54\,800$, $Pr = 6500$, $T_h = 32.6°C$, $T_c = 19.3°C$, Hallcrest liquid crystals used for experiment, (b) $Ra = 96\,000$, $Pr = 5100$, $T_h = 38°C$, $T_c = 20°C$, BDH Chemicals liquid crystals and Plexiglass particles used for experiment and (c) $Ra = 364\,000$, $Pr = 2700$, $T_h = 55.3°C$, $T_c = 20.1°C$, Hallcrest liquid crystals used for experiment.

Fig. 4. Experimental and numerical results for the enclosure with partition: (a) $Ra = 96\,000$, $Pr = 5100$, $T_h = 38°C$, $T_c = 20°C$, BDH Chemicals liquid crystals and Plexiglass particles used for experiment, (b) $Ra = 182\,000$, $Pr = 3900$, $T_h = 45.5°C$, $T_c = 19.3°C$, Hallcrest liquid crystals used for experiment and (c) $Ra = 258\,000$, $Pr = 3300$, $T_h = 50.2°C$, $T_c = 19.3°C$, Hallcrest liquid crystals used for experiment.

duced with the liquid crystals the uncertainty in the dynamic viscosity is ±10%.

A uniform collocated grid with 76 × 76 control volume cells was used for the enclosure without partition. In each half of the partitioned enclosure a uniform grid with 76 cells in the vertical direction and 36 cells in the horizontal direction was used. Eight uniform cells in the horizontal direction were used inside the partition. For the convective terms the central difference scheme was used with the "deferred correction" similar to that in Khosla and Rubin (1974), while the diffusion terms were approximated by using a second order central difference approximation.

The SIMPLE procedure (Patankar and Spalding, 1972) was used to solve the set of equations. The convergence criterion was that the average mass imbalance has to be smaller then 10^{-9}. Also, the changes of temperature and average Nusselt numbers were monitored from iteration to iteration. More details about the numerical procedure, convergence history and results can be found in Cuckovic-Dzodzo, (1996) and Cuckovic-Dzodzo et al. (1996a and 1998). To verify the derived numerical procedure, the results for the enclosure without partition filled with air (but with temperature dependent properties) were compared with the bench mark results of de Vahl Davis (1983) and Hortmann et al. (1990), obtained with the Boussinesq approximation. The maximum difference of the average Nusselt numbers occured for the maximum value of the Rayleigh number ($Ra = 10^6$), but it was less than 2.7%.

4. Discussion of the results

The experimentally and numerically obtained velocity and temperature fields in the middle vertical plane of the enclosures without and with partition are presented for various Rayleigh numbers in Figs. 3 and 4, respectively.

The experimentally obtained particle streak lines in the enclosure without partition can be compared with the numerically obtained stream lines in Fig. 3. The transition of the flow patterns from one central eddy towards two eddies with the increase of the Rayleigh number is in agreement with the previous results (Elder, 1965a, b). Increasing the Rayleigh number causes the eddy centers to move towards the vertical sides due to the decrease of thickness of the velocity boundary layers (compare cases for $Ra = 96\,000$ and $Ra = 364\,000$).

The numerically obtained vertical components of the velocity at the horizontal planes ($y = H/4$, $y = H/2$ and $y = 3H/4$) can be compared with the experimental results (symbols) in Fig. 5. It can be concluded that the results are in quantitative agreement. The discrepancy between numerical and experimental results can be explained due to the uncertainties of the velocity measurement as well as the uncertainty of the applied dynamic viscosity for the numerical model. Comparison of the numerically obtained velocity profiles in three horizontal cross-sections shows that the maximum vertical components of velocities occur at the middle cross-section and that the velocity boundary layers near the hot and cold walls grow in the direction of flow. Note that the numerically obtained velocity profiles are not symmetrical (as they would have been if the Boussinesq approximation had been applied). The maxima of the velocities in the cooler half of the enclosure are smaller due to the higher viscosity. Hence, it is obvious that the introduction of the model with variable fluid properties has a considerable bearing on the agreement of the numerical results with the experimental ones.

The distribution of the local Nusselt numbers near the vertical walls is presented in Fig. 6. For the same value of Rayleigh number the distribution of the local Nusselt numbers near the hot and cold vertical walls is not symmetrical. The maximum values of the local Nusselt numbers are different due to the different thickness of the boundary layers near the hot and cold vertical walls. The smaller viscosity near the hot vertical walls causes a decrease of the velocity boundary layer thickness and an increase of the maxima of the local Nusselt numbers, which occurs near the lower corner due to the penetration of the horizontal cold stream. The decrease of the thickness of the thermal boundary layers with the increase of the Rayleigh number results in higher values of the local and average Nusselt numbers.

Figs. 4, 7 and 8 present the corresponding results for the enclosure with the partition. The velocity and temperature fields are presented in Fig. 4. In each portion of the enclosure only one eddy is present. The positions of the centers of the eddies approach the horizontal plane $y = H/2$ as the Rayleigh number increases. For smaller values of the Rayleigh numbers the center of the eddy is below $y = H/2$ in the hot portion of the enclosure, and above $y = H/2$ in the cold portion of the enclosure. The same effect of the Rayleigh number increase on the position of the eddy centers was reported by Ho and Yih (1987) for narrow partitioned rectangular enclosures filled with air. The positions of the centers are dependent on the thickness of the boundary layers. The thickness of the boundary layers are increasing along the hot and cold vertical sides in the direction of the fluid flow. For smaller values of the Rayleigh numbers the thicknesses of the boundary layers are larger and the eddy centers are closer to the regions where the development of the boundary layers starts (in the lower and upper corners of the hot and cold portions of the enclosure, respectively).

The positions of the numerically and experimentally obtained isotherm lines can be compared in Fig. 4. It can be concluded that the shapes of the experimentally and numerically obtained isotherms are in good qualitative agreement. The quantitative discrepancy of the isotherm positions could be explained through the inability to supply correct boundary conditions for the transparent walls (horizontal sides in the numerical model), the influence of three-dimensional effects (front and back walls), the uncertainty of the applied dynamic viscosity, or the uncertainty of the color–temperature calibration of the liquid crystals (effects of lighting or view angles, see Lattime (1995)).

The vertical velocity profiles at the various horizontal cross-sections and vertical planes 2 and 3 are presented in Fig. 7. It can be concluded that experimental results in both vertical planes (planes 2 and 3 in Fig. 1) are in good quantitative agreement with numerical results, which supports the assumption of two-dimensional flow and heat transfer. The maximum vertical components of velocities occur at the middle cross-section, and velocity boundary layers near the hot and cold walls grow in the direction of flow, as in the enclosure

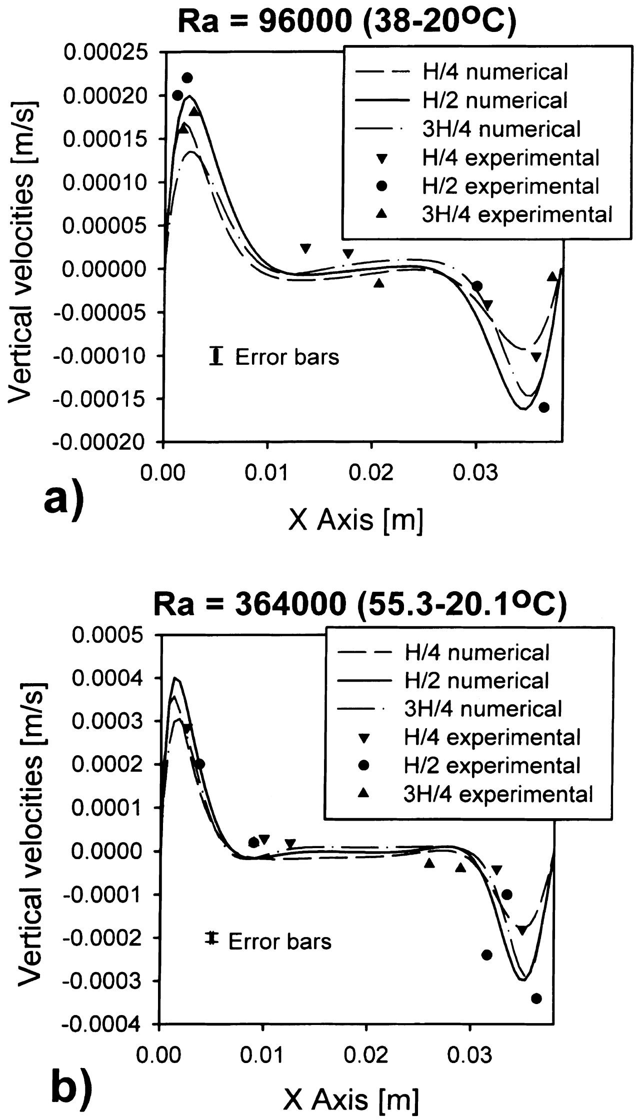

Fig. 5. Comparison of the experimentally and numerically obtained vertical velocities in various horizontal planes for: (a) $Ra = 96\,000$, $Pr = 5100$, $T_h = 38°C$, $T_c = 20°C$ and (b) $Ra = 364\,000$, $Pr = 2700$, $T_h = 55.3°C$, $T_c = 20.1°C$.

without partition. The thickness of the boundary layers near the vertical partitions are almost the same for all three horizontal cross-sections, due to the variable temperature of the partition surfaces. A comparison of the velocities and boundary layer thickness in the hot and cold portions of the enclosure shows that convection heat transfer effects are stronger in the hot portion of the enclosure, due to the smaller viscosity. This effect can be observed by comparing the local Nusselt numbers at the hot and cold vertical sides presented in Fig. 8.

The comparison of the various average Nusselt number correlations for enclosures without and with partition and various fluids is presented in Fig. 9. The average Nusselt number correlation based on isothermal partition models is:

$$\overline{Nu} = 0.339 Ra^{1/4} (H/W)^{-1/4} (N+1)^{-5/4}. \qquad (11)$$

This correlation is based on Duxbury (1979) and Nakamura et al. (1984) results for air-filled enclosures. The correlation is in agreement with the correlation developed by Churchill and Ozoe (see Churchill, 1983) for the unpartioned enclosures

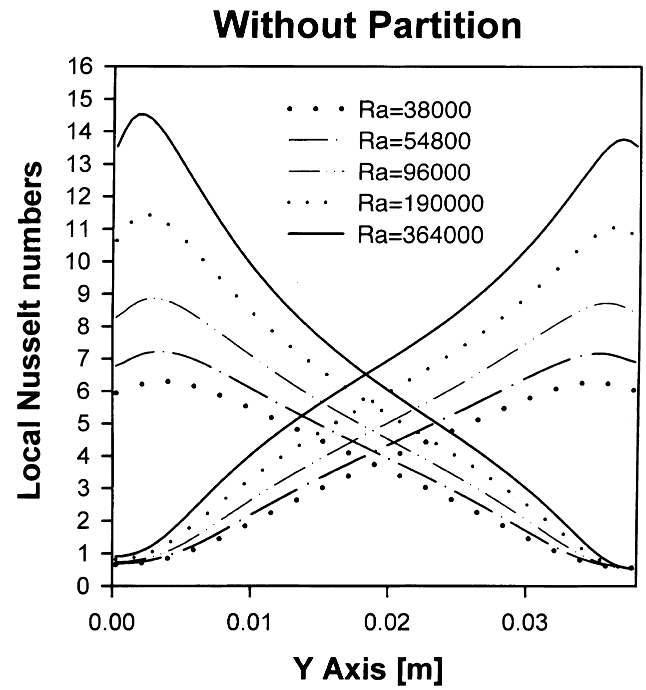

Fig. 6. Distribution of the local Nusselt numbers along the hot and cold vertical walls.

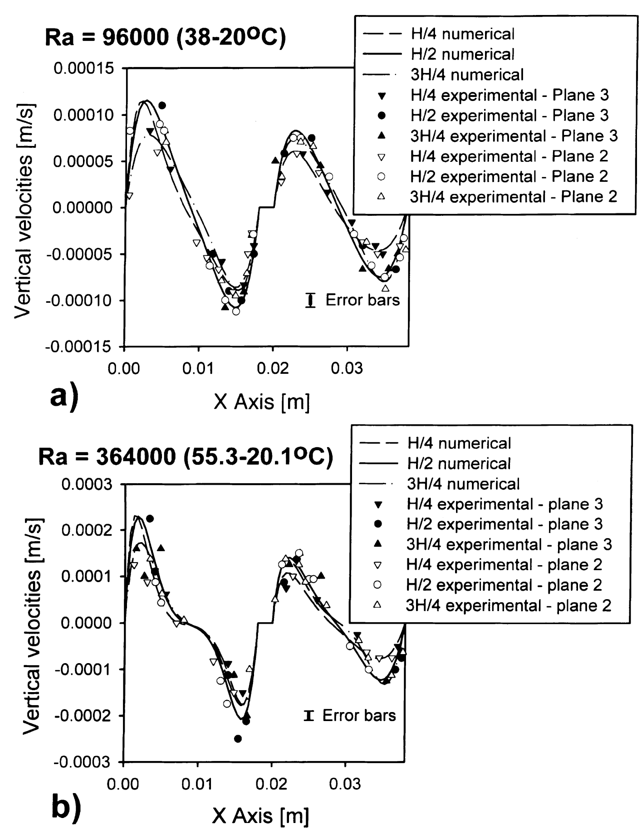

Fig. 7. Comparison of the experimentally and numerically obtained vertical velocities in various horizontal planes for: (a) $Ra = 96\,000$, $Pr = 5100$, $T_h = 38°C$, $T_c = 20°C$ and (b) $Ra = 364\,000$, $Pr = 2700$, $T_h = 55.3°C$, $T_c = 20.1°C$.

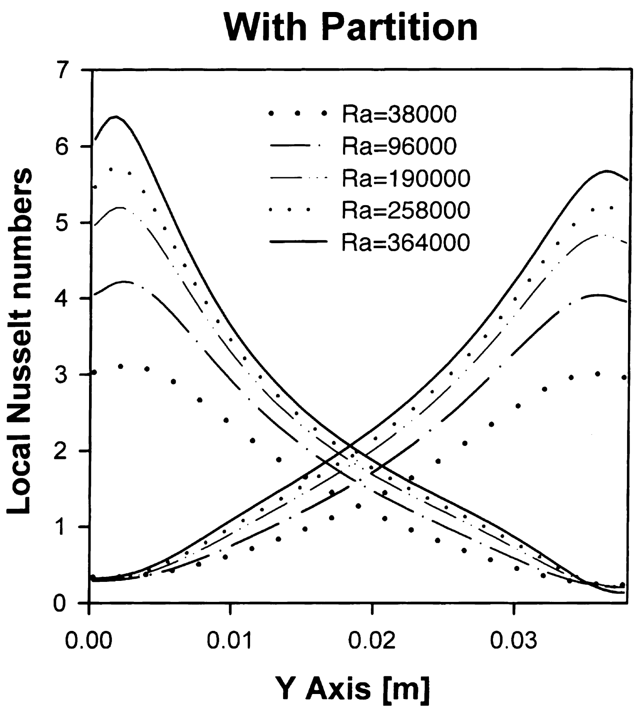

Fig. 8. Distribution of the local Nusselt numbers along the hot and cold vertical walls.

($N = 0$) with large H/W aspect ratios, which is based on the laminar boundary layer solution of Bejan (1979). The correlation (11) was used by Nishimura et al. (1988) for comparison with their correlation developed for water and valid for air:

$$\overline{Nu} = 0.297 Ra^{1/4} (H/W)^{-1/4} (N+1)^{-1}. \tag{12}$$

The correlation derived by Anderson and Bejan (1981) for water is:

$$\overline{Nu} = 0.167 Ra^{1/4} (N+1)^{-0.61}. \tag{13}$$

For the working fluid in the present paper, glycerol, two correlations are derived. The first one has the same form as correlations for air and water.

$$\overline{Nu} = 0.201 Ra^{0.276} (N+1)^{-1.4}. \tag{14}$$

The second correlation, more in the scope of the present paper, takes into account the influence of the variable fluid properties by using the Prandtl numbers near the hot and cold walls (Pr_h and Pr_c).

$$\overline{Nu} = 0.0512 Ra^{0.421} (N+1)^{-1.4} \left(\frac{Pr_c}{Pr_h}\right)^{-0.207}. \tag{15}$$

It is evident that the involving of the new dimensionless parameter Pr_c/Pr_h has changed the Rayleigh number exponent. Correlations are valid in the range of Rayleigh numbers $38\,000 < Ra < 369\,000$ and Prandtl numbers $2700 < Pr < 7000$. All properties, including Rayleigh and Prandtl numbers, are calculated based on the average fluid temperature T_0, except Prandtl numbers near the hot and cold vertical walls Pr_h and Pr_c in Eq. (15), which are based on corresponding temperatures T_h and T_c. The temperature of the cold wall was in all cases close to 20°C (19.3°C < T_c < 20.1°C). Rayleigh and Prandtl numbers were changed by increasing the hot wall temperature T_h (32.6°C < T_c < 55.6°C). The validity of the correlations for other fluids with a nonlinear dependence of the properties remains to be tested.

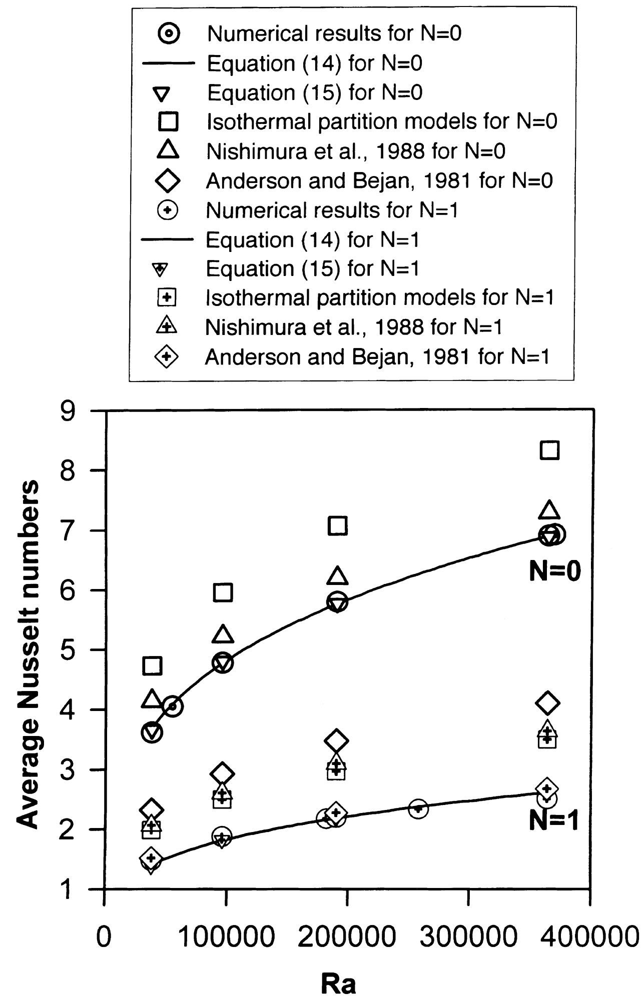

Fig. 9. The average Nusselt number dependence on average Rayleigh number for the enclosures without ($N = 0$) and with ($N = 1$) partition.

The difference in average Nusselt numbers obtained from Eqs. (14) and (15) is small because both correlations are curve fits of the numerically obtained average Nusselt numbers (also presented in Fig. 9). Eq. (14) and obtained coefficients are similar to the previously developed correlations for air and water. Eq. (15) takes into account various properties, and due to the variation of Pr_h and Pr_c values the coefficients are different than in (14).

The developed correlations (for glycerol) are in best agreement with Nishimura et al. (1988) and Anderson and Bejan (1981) correlations for enclosures without and with partition, respectively. The comparison of the average Nusselt numbers for enclosures without and with partition indicates that the introduction of a complete vertical partition reduces convective heat transfer from 59.1% to 63.6% in the range of Rayleigh numbers $38\,000 < Ra < 369\,000$. Fig. 9 shows that previously tested enclosures with water and air exhibits similar heat transfer reduction.

5. Conclusion

The visualization of the temperature and velocity fields of laminar natural convection in enclosures without and with partition was performed both experimentally and numerically. The fluid used in the experiment and numerical calculation was glycerol.

Thermochromic liquid crystals and Plexiglass particles were used to visualize the temperature and velocity fields, respectively. The experimental results were used to verify the numerical model which takes into account the dependence of the thermophysical properties on temperature. A good agreement between the experimental and numerical results for glycerol as working fluid was achieved. Numerically obtained velocity profiles are in close agreement with the experimental ones. The experimentally and numerically obtained shapes of isotherms are in agreement. The quantitative differences of the experimentally and numerically obtained isotherms remain to be explained.

The conclusion is that the introduction of a complete vertical partition reduces convective heat transfer from 59.1% to 63.6% in the range of Rayleigh numbers $38\,000 < Ra < 369\,000$. This is in good qualitative agreement with the previous results obtained with water and air by the other authors. However, the correlations for the average Nusselt numbers are slightly different from the previous correlations valid for air and water.

Acknowledgements

The authors are grateful to Professor M.J. Braun (The University of Akron, Mechanical Engineering Department) who offered the opportunity to finish this work by allocating the necessary laboratory equipment and computer facilities. Partial financial support from the Faculty research grant No: 2-07289 (The University of Akron) allocated to M.B. Dzodzo is acknowledged as well.

References

Acharya, S., Tsang, C.H., 1985. Natural convection in a fully partitioned, inclined enclosure. Numer. Heat Transfer 8, 407–428.

Anderson, R., Bejan, A., 1981. Heat transfer through single and double vertical walls in natural convection: theory and experiment. Int. J. Heat and Mass Transfer 24, 1611–1620.

Bejan, A., 1979. Note on Gill's solution for free convection in a vertical enclosure. J. Fluid Mech. 90, 561–568.

Catton, I. 1978. Natural convection in enclosures. Proceedings of the Sixth International Heat Transfer Conference, vol. 6, pp. 13–43.

Churchill, S.W., 1983. Free convection in layers and enclosures. In Heat Exchanger Design Handbook, Chapter 2.5.8, Hemisphere, Washington, DC.

Ciofalo, M., Karayiannis, T.G., 1991. Natural convection heat transfer in a partially or completely-partitioned vertical rectangular enclosure. Int. J. Heat and Mass Transfer 34, 167–179.

Cuckovic-Dzodzo, D.M., 1996. Effects of heat conducting partition on laminar natural convection in an enclosure. M.Sc. Thesis, Department of Mechanical Engineering, The University of Belgrade.

Cuckovic-Dzodzo, D.M., Dzodzo, M.B., Pavlovic, M.D., 1996a. Influence of heat conducting partition on free laminar convective flow in a plane enclosure. In: Proceedings of the Second International Symposium – Contemporary Problems of Fluid Mechanics, Yugoslav Society of Mechanics, Belgrade, pp. 249–252.

Cuckovic-Dzodzo, D.M., Dzodzo, M.B., Pavlovic, M.D., 1996b. Visualization of laminar natural convection in a cubical enclosure with partition. FED-Vol 239, 1996, ASME Fluids Engineering Division Conference vol. 4, San Diego, pp. 225–230.

Cuckovic-Dzodzo, D.M., Dzodzo, M.B., Pavlovic, M.D., 1998. A mathematical model and numerical solution for the conjugated heat transfer in a fully partitioned enclosure containing the fluids with variable nonlinear thermophysical properties. In: Theoretical and Applied Mechanics, Yugoslav Society of Mechanics, vol. 24, pp. 29–54.

de Vahl Davis, G., Jones, I.P., 1983. Natural convection in a square cavity: a comparison exercise. Int. J. Numer. Meth. Fluids 3, 227–248.

de Vahl Davis, G., 1983. Natural convection of air in a square cavity: a bench mark numerical solution. Int. J. Numer. Meth. Fluids 3, 249–264.

Duxbury, D., 1979. An Interferometric study of natural convection in enclosed plane air layers with complete and partial central vertical divisions. Ph.D. Thesis, University of Salford.

Dzodzo, M.B., 1991. Laminar natural convection in some enclosures of arbitrary cross-section. Ph.D. Thesis, Department of Mechanical Engineering, The University of Belgrade.

Dzodzo, M.B., 1993. Visualization of laminar natural convection in romb-shaped enclosures by means of liquid crystals. In: Sideman S., Hijikata K., Yang W. J. (Eds.), Imaging in Transport Processes, Begel House Publishers, pp. 183–193.

Dzodzo, M.B., Braun, M.J., Lattime, S.B., 1994. A non-intrusive computer automated investigation of natural convection using thermochromic liquid crystals and comparison with numerical simulation. In: Heat Transfer 1994 – Proceedings of the Tenth International Heat Transfer Conference, vol. 2, Brighton, UK, pp. 225–230.

Elder, J.W., 1965a. Laminar free convection in a vertical slot. J. Fluid Mech. 23(1), 77–98.

Elder, J.W., 1965b. Turbulent free convection in a vertical slot. J. Fluid Mech. 23(1), 99–111.

Elder, J.W., 1966. Numerical experiments with free convection in a vertical slot. J. Fluid Mech. 24(4), 823–843.

Gray, D.D., Giorgini, A., 1976. The validity of the Boussinesq approximation for liquids and gases. Int. J. Heat and Mass Transfer 19, 545–551.

Hallcrest, Inc., 1991. An Introduction to Thermochromic Liquid Crystals.

Hiller, W.J., Koch, St., Kowalewski, T.A., 1989. Three-dimensional structures in laminar natural convection in a cube enclosure. Exp. Therm. Fluid Sci. 2, 34–44.

Ho, C.J., Yih, Y.L., 1987. Conjugate natural convection heat transfer in an air-filled rectangular cavity. Int. Commun. Heat and Mass Transfer 14, 91–100.

Hortmann, M., Peric, M., Scheurerer, G., 1990. Finite volume multigrid prediction of laminar natural convection: bench-mark solutions. Int. J. Numer. Meth. Fluids 11, 189–207.

Kangni, A., BenYedder, R., Bilgen, E., 1991. Natural convection and conduction in enclosures with multiple vertical partitions. Int. J. Heat and Mass Transfer 34, 2819–2825.

Karayiannis, T.G., Ciofalo, M., Barbaro, G., 1992. On natural convection in a single and two zone rectangular enclosure. Int. J. Heat and Mass Transfer 35, 1645–1657.

Khosla, P.K., Rubin, S.G., 1974. A diagonally dominant second-order accurate implicit scheme. Computers and Fluids 2, 207–209.

Lattime, S.B., 1995. Thermochromic liquid crystal applications in a quantitative study of laminar natural and forced convection heat transfer. M.Sc. Thesis, Department of Mechanical Engineering, The University of Akron.

Lattime, S.B., Braun, M.J., Dzodzo, M.B. 1995. Simultaneous visualization of flow and temperature patterns in a shell and tube heat exchanger by TLC. FED-vol. 218, 1995, ASME/JSME Fluids Engineering and Laser Anemometry Conference and Exibition, Hilton Head, South Carolina, pp. 7–14.

Mamou, M., Hasnaoui, M., Vasseur, P., Bilgen, E., 1994. Natural convection heat transfer in inclined enclosures with multiple conducting solid partitions. Numerical Heat Transfer A, 25, 295–315.

Nakamura, H., Asako, Y., Hirata, T., 1984. Natural convection and thermal radiation in enclosures with partition plate. Trans. JSME Ser. B 50, 2647–2654.

Nishimura, T., Shiraishi, M., Kawamura, Y., 1987. Natural convection heat transfer in enclosures with an off-center partition. Int. J. Heat and Mass Transfer 30, 1756–1758.

Nishimura, T., Shiraishi, M., Nagasawa, F., Kawamura, Y., 1988. Natural convection heat transfer in enclosures with multiple vertical partitions. Int. J. Heat and Mass Transfer 31, 1679–1686.
Ostrach, S., 1972. Natural convection in enclosures. In: Hartnett J.P., Irvine T.F. (Eds.), Advances in Heat Transfer, Academic Press, New York, p. 1.
Ostrach, S., 1982. Natural convection heat transfer in cavities and cells. Heat Transfer 82(1), 365–379, Munchen.
Parsley, M., 1991. The use of thermochromic liquid crystals in research applications, thermal maping and non-destructive testing. In: Proceedings of the Seventh IEE Semi-Therm Symposium, pp. 53–58.
Patankar, S.V., Spalding, D.B., 1972. A calculation procedure for heat, mass and momentum transfer in three-dimensional parabolic flows. Int. J. Heat Mass Transfer 15, 1787–1806.
Penot, F., N'Dame, A., 1992. Successive bifurcations of natural convection in a vertical enclosure heated from the side. In: Third UK National Conference incorporating First European Conference on Thermal Sciences, Institution of Chemical Engineers, vol. 1, Hemisphere, Washington, DC, pp. 507–513.
Tong, T.W., Gerner, F.M., 1986. Natural convection in partitioned air-filled rectangular enclosures. Int. Commun. Heat and Mass Transfer 13, 99–108.
Toulokian, Y.S., Liley, P.E., Saxena, S.C. (Eds.), 1970a. Thermophysical properties of matter. Thermal Conductivity Nonmetallic Solids, vol. 3, The TPRC Data Series, IFI/Plenum Press, New York.
Toulokian, Y.S., Powell, R.W., Ho, C.Y., Klemens P.G. (Eds.), 1970b. Thermophysical properties of matter. Thermal Conductivity Nonmetallic Liquids and Gases, vol. 2, The TPRC Data Series, IFI/Plenum, New York.
Toulokian, Y.S., Makita, T. (Eds.), 1970. Thermophysical properties of matter. Specific Heat Nonmetallic Liquids and Gases, vol. 6, The TPRC Data Series, IFI/Plenum, New York.
Yang, K.T., 1987. Natural convection in enclosures. In: Kakac, S., Shah, R.K., Aung, W., (Eds.), Handbook of Single-Phase Convective Heat Transfer, Wiley, New York, pp. 13-1–13-51.